81-5-97
高工研図書室

DEUTSCHES ELEKTRONEN-SYNCHROTRON DESY

DESY 81-017
April 1981

MEASURING THE CHARGES OF QCD JETS

by

C. J. Maxwell
Rutherford Laboratory

M. J. Teper
Deutsches Elektronen-Synchrotron DESY, Hamburg

NOTKESTRASSE 85 · 2 HAMBURG 52

DESY behält sich alle Rechte für den Fall der Schutzrechtserteilung und für die wirtschaftliche Verwertung der in diesem Bericht enthaltenen Informationen vor.

DESY reserves all rights for commercial use of information included in this report, especially in case of apply for or grant of patents.

To be sure that your preprints are promptly included in the
HIGH ENERGY PHYSICS INDEX ,
send them to the following address (if possible by air mail) :

DESY
Bibliothek
Notkestrasse 85
2 Hamburg 52
Germany

DESY 81-017
April 1981

Measuring the charges of QCD jets

C.J. Maxwell

Rutherford Laboratory

M.J. Teper

Deutsches Elektronen-Synchrotron DESY

Abstract

We investigate the effects of perturbative branching upon the accuracy with which one can determine the charge of the underlying QCD quantum from the charge structure of a given hadronic jet. We show explicitly how at asymptotic Q^2 we lose all such charge information. We investigate these effects at current PETRA energies using the Monte Carlo program of Fox and Wolfram; and find that a reasonably accurate charge determination is still possible at these energies. We suggest the variation of the jet charge structure with multiplicity, at a given energy, as a sensitive probe of the onset of perturbative branching inside jets.

1. Introduction

The problem of indentifying the charge of the QCD quantum that gives rise to a given jet of hadrons is clearly important. In two previous papers [1,2] we have shown how to construct charge measures that are insensitive to charge fluctuations arising during the soft hadronisation. In this paper we investigate how the accuracy of such charge measures is affected by perturbative bremsstrahlung.

We shall work throughout in the leading logarithm approximation (LLA) [3], or close variants there-of, both in our analytic calculations and in our numerical calculations where we use the jet Monte Carlo program of Fox and Wolfram [4,5].

First we review the derivation of the charge measure of ref. (2) for soft jets, and point out the qualitative impact of perturbative branching. We follow this with a quantitative picture of quark jets at very high Q^2. We illustrate all this with a quark jet possessing an energy of about 10^{15} GeV - the grand unification (GUTS) scale. We then explicitly demonstrate how at truly asymptotic Q^2 all charge information (event-by-event) is lost.

Having clarified what happens at very high Q^2, we return to the practical question of what happens at PETRA energies. At such intermediate energies analytic calculations are unlikely to be reliable, so we perform our calculations with the Fox and Wolfram Monte Carlo [4] which contains both (modified) LLA perturbative branching and subsequent hadronisation. We shall find that the perturbative aspect is indeed important at PETRA energies; nonetheless

the reliability of our charge measure is in fact roughly as good as was estimated in our previous work [2], so that we can expect to be able to infer the quark charge reliably in most events.

2. A confinement-safe charge measure

In this section we briefly describe the charge measure that was introduced in refs. (1,2). The reader should consult those references for further details [6].

Consider a jet of hadrons produced from some initial quark, q. We suppose this jet to be dominated by the soft hadronisation process so that its properties are similar to those of the jets observed in ordinary soft hadronic collisions. In particular assume (i) the jet possesses short range charge correlations (SRCC); (ii) a uniform and finite density of hadrons in rapidity (away from the fragmentation region); (iii) a leading particle effect; and (iv) small transverse momenta.

We label the hadrons in the jet by their rapidities. In units of rapidity let the charge correlation length be l_c (which we expect to be about 1 or 2 units). Break up the rapidity interval occupied by the jet into adjacent sections of length l_c as in Fig. 1. Label the faces of these sections 1,2,...,M as shown, and their rapidities by y(1), ..., y(M). Now, consider the net charge of the hadrons with $y > y(i)$; call it Q(q;i). This net charge will equal the charge of q (since by the leading particle effect the quark q should lie in one of the fastest hadrons, with $y > y(i)$) plus the charge flowing from the part of the event with $y < y(i)$ into the part of the jet with $y > y(i)$. Since the

hadrons with $y > y(i)$ have net mesonic quantum numbers (disregarding the unlikely case that y(i) separates a baryon antibaryon pair) this charge flow across y = y(i) will consist of an antiquark charge plus some integer valued charge fluctuation centred about zero. So we have

$$Q(q;i) = q + \langle \bar{q} \rangle \pm \sigma \qquad (1)$$

where σ is the standard deviation of the zero-centred charge fluctuation. Now by SRCC the σ fluctuations across different boundaries i and j are independent, so if we average Q(q;i) from i = 1 to M we obtain

$$Q_M(q) = \frac{1}{M} \sum_{i=1}^{M} Q(q;i)$$
$$= q + \langle \bar{q} \rangle \pm \frac{\sigma}{\sqrt{M}} \qquad (2)$$

This is the simplest version of the charge measure introduced in refs. (1,2). Note that it is designed to be applied to a single jet, rather than averaged over many events, and note also how the precision of the measure increases rapidly with M. $\bar{q}$ is of course calculable; in the case when we only include $\bar{u}$ and $\bar{d}$ we have $\langle \bar{q} \rangle = -\frac{1}{6}$.

Now in the above we assumed that the incident quark always ends up in a hadron with $y > y(i)$ for any i. In reality there will be some probability for this quark to be slowed down below y = y(i). Call this probability $P_q(W_i)$ where $\frac{1}{2}W_i$ is the energy of the portion of the jet with $y > y(i)$ in a frame where y(i) = 0. By the leading particle hypothesis $P_q(W_i)$ should fall rapidly with increasing W_i; and indeed an analysis [7] of ν and $\bar{\nu}$ data [8] suggests

that at moderate Q^2,

$$P_q(W_i) \approx \frac{1.4}{W_i} \qquad (3)$$

for W_i not too small. It is also possible that σ should vary with i, in which case we must use $\sigma(i)$ in our calculations. We then find that the appropriate generalisation of (2) is

$$Q_M(q) = \sum_{i=1}^{M} Q(q;i)\,\frac{[1-P_q(W_i)]}{\sigma^2(i)} \cdot \left\{\sum_{i=1}^{M}\frac{[1-P_q(W_i)]}{\sigma^2(i)}\right\}^{-1}$$

$$= q + \langle\bar{q}\rangle \pm \left\{\sum_{i=1}^{M}\frac{[1-P_q(W_i)]^2}{\sigma^2(i)}\right\}^{-1/2} \qquad (4)$$

Note the way the terms in the above sum are weighted. A given term Q(q,i) will contribute the less to the charge measure the smaller the probability that it contains the initial quark, i.e. the larger is $P_q(W_i)$; and also the larger is the random fluctuation $\sigma(i)$. This is just common-sense; in addition the charge measure of eqn. (4) is designed to be the "best possible" measure given our assumptions.

We now turn to a preliminary discussion of the expected effects of perturbative branching upon our four initial assumptions and the consequent accuracy of the charge measure.

(i) We expect that the SRCC property of the soft hadronisation should be unaffected by any prior perturbative branching. However, the branching process itself violates SRCC: a quark antiquark pair produced early on in the branching will, at the point prior to hadronisation, be far apart in phase space and hence will end up in hadrons far apart in phase space. If one hadron is at y(I) and the other at y(J) then we see that the extra error induced in the charge measure, eqn. (2), is

$$\delta Q_M(q) \approx \frac{I-J}{M} \times \text{quark charge} \qquad (5)$$

So if I-J is comparable to M the measure loses all precision.

(ii) Perturbative branching increases the number of quarks and gluons that hadronise in a given jet and hence will increase the density of hadrons per 1_c interval; call it n(i). We expect $\sigma(i) \propto \sqrt{n(i)}$, and we see from (4) that the error on the charge measure increases as

$$\delta Q_M(q) \propto n^{1/2} \qquad (6)$$

(iii) Perturbative bremsstrahlung implies that the incident quark loses momentum before hadronisation. This weakens the leading particle effect in the quark jet, reducing the coefficients $[1 - P_q(W_i)]$ in (4), with an effect on the error that one can see quantitatively in (4).

(iv) The transverse momenta in a jet increase with increasing perturbative branching. This does not directly affect our charge measure, but it will in general falsify our claim that this is the "best possible" charge measure.

When a jet grows in the transverse as well as in the longitudinal directions, SRCC implies that it can be decomposed three dimensionally into boxes of length l_c such that charge fluctuations across the faces of different boxes are independent whatever their orientation. We can still apply our one dimensional measure to such a jet but it is clear that we are then only using a little of the information provided by SRCC and should expect that better measures will be possible.

3. Properties of QCD jets

In developing a semi-quantitative understanding of the way QCD jets develop we shall work within the leading log approximation [3] (LLA). While this should give us a good insight into how things change with Q^2, the reader should beware of taking the results too literally at the quantitative level. For example the rapid multiplicity increase with Q^2 shall be one of our primary concerns; but the detailed LLA prediction [9] is not expected to be accurate [10]. This arises because the average multiplicity has the schematic form [9]

$$\langle n \rangle \sim \exp(a\sqrt{\ln Q^2}) \tag{7}$$

so that the average x is

$$\langle x \rangle \sim \langle n \rangle^{-1} \sim \exp(-a\sqrt{\ln Q^2}) \tag{8}$$

and hence

$$\ln^2 \langle x \rangle \sim \ln Q^2 \tag{9}$$

Thus factors of $\ln Q^2$ can be outweighed by factors of $(\ln x)^2$ and lower order terms are important. This will change the parameter a from the LLA result, but the form of (7) will probably remain unchanged [10]. This illustrates our earlier caution.

We shall use the LLA to tell us how a quark of virtuality $\sim Q^2$ turns into a "jet" of quarks and gluons of virtuality $Q_o^2 \sim 1\ \mathrm{GeV}^2$, which is the lowest Q_o^2 at which we can pretend to have any confidence in the LLA. The LLA development of a QCD jet is very slow, being primarily governed by the variable

($N_{c,f}$ = no. colours, flavours)

$$Y = \frac{6}{11N_c - 2N_f} \log\left[\frac{\alpha_s(\mu^2)}{\alpha_s(Q^2)}\right]$$

$$= \frac{6}{11N_c - 2N_f} \log\left[\frac{1}{\alpha_s(Q^2)}\right] \tag{10}$$

where we have taken (as we shall continue to do from now on) $\mu^2 = Q_o^2$ and $\alpha_s(Q_o^2) = 1$, which corresponds to $\Lambda \approx 500$ MeV. (We shall for simplicity be careless about the fact that N_f increases with Q^2). Of course, we are primarily interested in the structure of the quark jet in terms of its final observable hadrons, rather than in terms of some intermediate partons. We shall make the conventional assumption that the number of hadrons is roughly proportional to the number of partons of virtuality $Q_o^2 \sim 1\ \mathrm{GeV}^2$, and also that the phase space distribution of these hadrons closely follows the distribution of the partons which is not an unreasonable assumption in any fragmentation/recombination picture of hadronisation.

We will now go through the list of assumptions (i) - (iii) that we made in Section 2 and see what happens in each case as Q^2 becomes large.

(i) Let $x_v(Q_c^2)$ be the fraction of its original momentum that the initial "valence" quark possesses when its virtuality has been degraded to Q_o^2. If Q^2 is small then $x_v(Q_o^2) \sim 1$, there is little perturbative branching, and the situation is essentially as in the naive parton model (to which our charge measure best applies) where any eventual slowing down of the quark occurs during the hadronisation stage. As Q^2 increases the LLA predicts that

$$\langle x_v \rangle = e^{-\frac{16}{9}Y} \approx [\alpha_s(Q^2)]^{0.46} \qquad (11)$$

This is a slow decrease (in going from PETRA to GUTS energies $\langle x_v \rangle$ decreases by about a factor of 4). Moreover the absolute decrease is in itself not particularly relevant to us; we are more interested in whether the number of hadrons which are faster than the hadron containing the valence quark increases with Q^2 or not. We translate this question into the corresponding question in terms of the quarks and gluons of virtuality $Q_o^2 \sim 1$ GeV^2. In ref. (3) an expression for the number of such non-valence quanta possessing $x > x_o$ has been derived for small x_o in the LLA. In our region of interest it may be approximated as

$$\langle n(x>x_o) \rangle = \frac{4}{9} \frac{e^{Z-5.6Y}}{\sqrt{2\pi Z}} \left\{ 1 + \frac{1}{8Z} + \frac{20}{3}\frac{Y}{Z}\left(1 - \frac{3}{8Z}\right) \right\} \qquad (12)$$

where

$$Z = 2\sqrt{6Y \log 1/x_o}$$

We plot $\langle n(x > \langle x_v \rangle) \rangle$ as a function of Y in Fig. 1. The main points are:

(a) up to GUTS energies $\langle n(x > \langle x_v \rangle) \rangle$ varies only slowly, and the valence quark is usually the fastest parton. (The precise numbers shown for PETRA/LEP energies are overestimates because the values of $\langle x_v \rangle$ at these energies are too large to allow the reliable use of (12)).

(b) $n(x > \langle x_v \rangle)$ does increase with Q^2 and eventually becomes very large. Here "eventually" $\gg$ GUTS! Of course, the separate treatment of QCD only makes sense below GUTS energies; so any discussion of higher Q^2 is not of any direct physical interest.

While the above tells us that for most events the valence quark is the leading parton, it does not tell us the width of the x_v distribution. In particular what is the probability that the valence quark finds itself slowed down to $x_v \sim 0$ just before hadronisation? We can find the leading power behaviour of the number density dn_v/dx_v near $x_v = 0$ by looking at the moments of the valence quark momentum distribution, $G_v(n,Y)$, which have the usual LLA expression [3]

$$G_v(n,Y) = e^{-A_n Y} \qquad (13)$$

where the A_n are the appropriate anomalous dimensions, and noting that the n at which $G_v(n,Y)$ first diverges as we decrease n reflects the leading power behaviour of dn_v/dx_v near $x_v = 0$. We find (leading power behaviour only)

$$\frac{dn_v}{dx_v} \underset{x_v \sim 0}{\sim} \text{const.} \qquad (14)$$

or, in terms of longitudinal rapidity, y,

$$\frac{dn_v}{dy} \sim e^{-|y-y_{max}|} \qquad (15)$$

Since we expect [2,7] that at the hadronisation stage the valence quark will develop a tail at low x_v that is at least as large as that given by eqn. (15) it is apparent that at all energies of any possible physical interest the initial quark's relative momentum distribution is such as not to seriously reduce the accuracy of our charge measure in (2) and (4).

(ii) Short range charge compensation - the idea that if there is a positively charged particle produced at some point in phase space in the jet, then the corresponding negative particle will be close in phase space, the correlation length being typically O(1) in units of rapidity (or its transverse generalisation), - is a well established and understood property of the jets produced in normal soft hadron-hadron collisions [11], and preliminary analyses [12] of quark jets confirm this expectation. So, as remarked earlier, a breakdown of SRCC at the hadronic level can only occur if $q\bar{q}$ pairs have managed to become distant in phase space prior to the hadronisation: then by SRCC the hadrons containing the q and $\bar{q}$ will be about as distant in phase space as were the q, $\bar{q}$ just before hadronisation. In a perturbative QCD jet this happens with the production of $q\bar{q}$ pairs early in the branching process

(i.e. pairs of a large virtuality). The corresponding q, $\bar{q}$ with a virtuality $Q_0^2 \sim 1\ \text{GeV}^2$ will have a large relative invariant mass $\sim O(Q/Q_0)$ and will be correspondingly distant in phase space. Of course $q\bar{q}$ production at a vertex characterized by virtuality $\sim \tilde{Q}^2$, will be suppressed relative to gluon production by a factor of $\propto (\tilde{Q}^2)$. However, the large number of vertices more than compensates for this. A crude calculation tells us that the first $q\bar{q}$ pair will be formed with a virtuality Q_L^2 that is $O(Q^2)$:

$$Q_L^2 \approx \frac{Q^2}{(\ln Q^2)^{2\sqrt{6/\alpha_s}}} \sim O(Q^2) \qquad (16)$$

so that the q and $\bar{q}$ will find themselves in hadrons that are very far apart in phase space.

Despite the serious breakdown of SRCC implied by all this, we now show that our charge measure is not much affected by the production of such $q\bar{q}$ pairs, because it turns out that the fractional momenta of q, $\bar{q}$ at $Q_0^2 \sim 1\ \text{GeV}^2$ are similar, and this is what is important in our charge measure.

So suppose that the $q\bar{q}$ pair is produced by a gluon of momentum fraction $\bar{x}$ and virtuality $\bar{Q}^2$. The $g \to q\bar{q}$ decay probability is not especially peaked, so the q and $\bar{q}$ at this stage carry comparable fractions of $\bar{x}$. By the time the q and $\bar{q}$ have degraded their virtuality to $Q_0^2 \sim 1\ \text{GeV}^2$, they will have average momentum fractions

$$\langle x_q \rangle \sim \langle x_{\bar{q}} \rangle \sim \frac{\bar{x}}{2} e^{-\frac{16}{9}\bar{y}} \qquad (17)$$

where we use eqn. (11) with $\bar{Y} = Y(\bar{Q}^2)$. Thus although $M_{q\bar{q}} \sim O(Q)$, longitudinally $x_q/x_{\bar{q}} \sim$ finite. This is not counterintuitive: consider a pair of massless quarks q, q' with opposite transverse momenta $p_\perp$, and with longitudinal momenta xP, x'P $\gg p_\perp$. Then if their invariant mass is $M_{q\bar{q}}$,

$$M^2_{q\bar{q}} = 2((x^2P^2+p_\perp^2)^{1/2}, xP, p_\perp)\ ((x'^2P^2+p_\perp^2)^{1/2}, x'P, -p_\perp)$$

$$\approx \left(\frac{x'}{x} + \frac{x}{x'} + 2\right)p_\perp^2 \qquad (18)$$

$$= \frac{(x+x')^2}{xx'}\ p_\perp^2 > 4p_\perp^2$$

So as long as the q, $\bar{q}$ longitudinal momenta are much bigger than their invariant mass (which is always true, at least by logarithms if not by powers of Q) we expect

$$x_q/x_{\bar{q}} \sim \text{finite} \qquad (19)$$

This expectation is confirmed by a more detailed examination of the shapes of the distributions in x_q and $x_{\bar{q}}$: the probability for $x_q/x_{\bar{q}} \leq \epsilon$ is proportional to ϵ for ϵ sufficiently small, so that the probability for the q and $\bar{q}$ to be very distant in phase space follows the functional form of the usual SRCC tail (as in eqn. (15)). A better estimate for $x_q/x_{\bar{q}}$, obtained by evaluating $(\langle x_q^2\rangle - \langle x_q\rangle^2)^{1/2}$ and hence the width of the x_q distribution, turns out to be roughly

$$x_q/x_{\bar{q}} \sim \left[\alpha_s(\bar{Q}^2)\right]^{-1/3} \qquad (20)$$

(assuming $x_q > x_{\bar{q}}$). So the longitudinal rapidity interval Δy between the q and $\bar{q}$ is typically

$$\Delta y \approx \left| \ln \frac{x_q}{x_{\bar{q}}} \right| \approx Y(\bar{Q}^2) \qquad (21)$$

which even at the highest energies is comparable to the correlation length of the usual short range correlations.

(iii) In the standard one-dimensional soft jet the density of particles per unit rapidity is more or less constant with rapidity and with energy: increasing multiplicity comes from the increasing range of rapidity available with increasing energy. So the charge fluctuations are also constant in rapidity and the error in our charge measure improves as $\frac{1}{\sqrt{N}}$, where N is the total multiplicity (see eqn. (2)). What happens in an asymptotic QCD jet? As we have seen, $\langle N\rangle \propto e^{a\sqrt{\ln Q^2}}$. Now the total rapidity length $\propto \ln Q^2$. Hence for at least some of the rapidity length

$$\frac{dN}{dy} \geq \frac{1}{\ln Q^2}\, e^{a\sqrt{\ln Q^2}} \xrightarrow[Q^2\to\infty]{} \infty \qquad (22)$$

and as argued in section 2 the corresponding fluctuations also become large:

$$\sigma(y) \propto \sqrt{\frac{dN}{dy}} \sim \frac{1}{\sqrt{\ln Q^2}} \; e^{\frac{a}{2}\sqrt{\ln Q^2}} \qquad (23)$$

Now, what is useful for picking out the incident quark is the portion of the jet slower than the incident quark, i.e. possessing $x < \langle x_v \rangle$. What is the particle density there? Asymptotically using eqns. (11) and (12) we see that $x \sim \langle x_v \rangle$ the density of particles is approximately

$$\frac{dn(x = \langle x_v \rangle)}{dy} \propto e^{Y} \qquad (24)$$

and increases with decreasing x. So the error in eqn. (4) is

$$\left[\sum_{i=1}^{\sim \ln Q^2} \frac{1}{\sigma^2(y_i)} \right]^{-1/2} \propto (\ln Q^2)^{\delta > 0} \qquad (25)$$

Thus we see explicitly that as Q^2 increases, the increasing density of particles eventually renders our charge measure useless. Of course,"eventually" may not mean much: surely the highest sensible energy for a QCD jet is the GUTS mass scale $\sim 10^{15}$ GeV. So we now exemplify all the above by calculating our charge measure for a typical quark jet of 10^{15} GeV, and we will estimate its error.

A GUTS jet

Consider a quark jet of energy $\sim 10^{15}$ GeV, originating from an off-shell quark of a similar virtuality. As we have seen, even at such an energy the initial quark is probably the leading parton just before hadronisation and the production of $q\bar{q}$ pairs has no degrading effect on such a longitudinal charge measure. So the main factor affecting the accuracy of our charge measure is the density of hadrons.

Using eqn. (12) we calculate the density of partons versus rapidity, $\frac{dn}{dy}$. As we remarked in section II the charge fluctuation increases as

$$\sigma(y) = \frac{1}{\beta} \sqrt{\frac{dn}{dy}} \qquad (26)$$

where β^{-2} is the conversion factor in going from partons of virtuality $\sim Q_o^2 = 1$ GeV^2, to the final hadrons. We plot the resulting $\beta\sigma(y)$ in Fig. 3. Now, in such a situation the best one can do (see section 2) is to pick one charged hadron per unit rapidity, and then the value of the charge measure becomes

$$Q(y) = \left(y - \frac{1}{6}\right) \pm \frac{\sigma}{\sqrt{\left\{ \sum_{i=1}^{\sim 3.5} \beta^2 \frac{dn}{dy_i} \right\}}} \qquad (27)$$

where previous estimates [2] give $\sigma \sim 1$. Reading the values off Fig. 3 gives us

$$Q(q) = q - \frac{1}{6} \pm \frac{\sigma}{\beta} \cdot \frac{1}{\sqrt{2 \cdot 14}} \qquad (28)$$

We expect $\sigma; \beta \sim O(1)$, so very roughly we find that applying our charge measure to a quark jet gives us the quark "charge" with an error of

$$\delta Q \approx \pm \frac{1}{\sqrt{2 \cdot 14}} \approx 0 \cdot 7 \qquad (29)$$

Thus the accuracy of the charge measure is poor - no better than one would obtain at the higher DORIS energies.

Note that if the jet had had a density of particles which was constant in rapidity and which was comparable to the density observed at low energies (as would be the case for a jet of energy 10^{15} GeV but virtuality 1 GeV) then the error would have been

$$\delta Q \sim \pm \frac{1}{\sqrt{35}} \sim \pm \cdot 17 \qquad (30)$$

since the length of the GUTS jet is about 35 rapidity units. The difference between (29) and (30) is a direct measure of the extent to which perturbative effects have degraded the charge information at the highest energy at which one can reasonably discuss QCD jets.

4. Loss of all charge information as $Q^2 \to \infty$

We have discussed above how the charge information in a QCD jet is degraded with increasing Q^2, at very high Q^2: this was quantitatively exemplified by an application of the charge measure of ref. (2) to a jet of energy 10^{15} GeV. However, it is clear that our 1 dim. charge measure does not utilize all the charge information available in an asymptotic QCD jet which is really 3 dimensional rather than just 1 dimensional (although in general longitudinal momenta remain much greater than transverse momenta): SRCC is reflected in the transverse charge structure of the jet just as it is in the longitudinal charge structure. We can accordingly generalize our partition of the 1 dimensional jet, as in Fig. 1b, to a corresponding partition of a 3 dimensional jet as in Fig. 4, where we show a 2 dimensional section of the jet. Each square has the dimensions of one charge correlation length, so that if there is a positively charged particle in one box it is compensated by a negative particle that is either in the same box or in a neighbouring box. There are charge fluctuations across all the various internal faces of this structure and if two faces are not too close SRCC assures us that the charge fluctuations across these faces are independent. Actually it is clear that our box-like decomposition is not the most appropriate: a honeycomb structure would be better. However, we stick to the simpler box picture since it will suffice. Note also the variables along the two axes: the longitudinal variable is just $\propto \ln p_\ell$ where p_ℓ is the longitudinal momentum, and on the transverse axes we have the transverse analogues, $\ln p_\perp$, where $p_\perp$ is the transverse momentum. The fact that SRCC implies a "box" like subdivision of phase space in these variables can be readily seen using the one dimensional character ($p_\ell \gg p_\perp$) of jets in the LLA.

The way SRCC localizes charge correlations in all directions invites us to construct a multidimensional generalization of our previous charge measure, which might perhaps be much more accurate at the (irrelevantly?) high Q^2 where we have seen that the 1 dimensional measure becomes poor. Of course, the production of $q\bar{q}$ pairs early in the perturbative showering will tend to disrupt any such multidimensional measure, because as we have seen such pairs will end up in hadrons that are distant from each other in phase space. In any case we shall not attempt any such generalizations in this paper.

What we wish to demonstrate in this section is that, quite independently of the charge measure employed, the charge information on an event by event basis is completely lost as $Q^2 \longrightarrow \infty$. To demonstrate this analytically we need to go to asymptotic values of the variables in the problem, such as Y. (This is not of course to imply that such Y are intended to be of physical interest: merely that the phenomena we wish to describe are obviously most easily derived when extrapolated to their extreme.)

For the first part of the argument consider the jet decomposed as in Fig. 4. Assume each box is populated with m charged hadrons. We wish to know: what is the probability that such a jet with a net charge q located somewhere near the front of the jet, would look like a neutral jet? Or, in other words, what is the probability that a neutral jet possesses a hadronic charge structure typical of a charged jet?

To see how to answer this question let us first pose it in the context of the simpler 1 dimensional model in Fig. 1b. We characterize the charge structure of the jet by the charge fluctuation across the sides of the boxes;

let $\sigma(i)$ be the fluctuation across the i'th side from the right. Let $\sigma_{nat}(i)$ be a "natural" random value of $\sigma(i)$. Suppose then we have a jet of charge q (residing in the fastest box) then for it to look like a typical neutral jet, whose charge fluctuations will be some typical $\sigma_{nat}(i)$, the actual charge fluctuations of this charged jet must all be shifted by q, away from their "natural" values:

$$\sigma(i) = \sigma_{nat}(i) - q \tag{31}$$

In the particularly simple case where

$$q^2 \gg \langle \sigma^2_{nat}(i) \rangle \tag{32}$$

we clearly will have a suppression factor, S, like

$$S = \left[P(\sigma = q) \right]^N \tag{33}$$

where N is the length of the jet (using the charge correlation length as a unit) and $P(\sigma = q)$ is the probability that a charge fluctuation takes the value q numerically. More generally, if we relax the condition (32), we expect S to have the form

$$S = \alpha^N \tag{34}$$

where α is some number less than one, simply because all the charge fluctuations across different sides are more or less independent. An interesting special case is for

$$q^2 \ll \langle \sigma_{rat}^2(i) \rangle \tag{35}$$

when, assuming a Gaussian form,

$$\frac{dN}{d\sigma} \propto e^{-\frac{\sigma^2}{2\langle\sigma^2\rangle}} \tag{36}$$

we see that

$$\alpha \sim e^{-q/\sqrt{\langle\sigma^2\rangle}} \tag{37}$$

So as $\langle\sigma^2\rangle$ increases, which typically will happen if the particle density increases, the probability for a charged jet to look like a neutral jet increases rapidly.

We will now extend this argument to the case of a fat jet as in Fig. 4. The central observation is that the neutral jet will look like a charge q jet if we can find a string of boxes from the front of the jet to the rear of the jet which looks like a (one-dimensional) q jet. Let the suppression factor across each face of such a one-dimensional string be α, and let L be the length of the string, then the total suppression will be

$$S = \sum \alpha^L \tag{38}$$

where $\sum$ represents the sum over all possible paths. When $S \gtrsim 1$ this means that the number of paths is so great as to overwhelm the individual suppression factor of α^L. Now, a typical path will take an equal number of steps in all

three directions, so if N is the number of boxes in the longitudinal direction (and assuming the jet is fat enough that we can neglect end effects) counting only the paths that never go backwards, we expect

$$L \sim 5^N \tag{39}$$

Now the total number of paths will be of the order

$$\text{number of paths} \sim 5^L \tag{40}$$

because at each box we can move out in 5 possible directions. So very crudely we can replace (38) by

$$S = (5\alpha)^L \tag{41}$$

Thus if $5\alpha > 1$, the suppression for any individual string is overwhelmed by the huge number of possible strings, and all charge information is lost. Our argument has been very crude, but doing better (e.g. using a honeycombed jet with more faces) merely serves to strengthen the result.

For a quark charge, q, we expect $\alpha > 1/5$ even for a soft jet. In a QCD jet since the number of boxes $\sim (\ln Q)^3$ while the total multiplicity $\sim \exp(a\sqrt{\ln Q^2})$, it is evident that the portion of the jet where nearly all of the multiplicity resides will have $\alpha \sim 1$ and will carry no charge information.

So we have seen that that portion of a QCD jet which carries most of the multiplicity carries no charge information: this certainly includes the portion

of the jet with

$$x_o \lesssim O(e^{-6Y}) \tag{42}$$

which we can see by asking when the average multiplicity per unit box necessarily starts growing. So the longitudinal rapidity range available for any charge measure is

$$\delta y \sim \ln x_o \sim \text{const.} \times Y \tag{43}$$

We have seen that there are $O(e^Y)$ partons faster than the initial quark. To maximise our chance of picking out the net jet charge we minimise the various charge fluctuations by assuming that the initial quark and the very fast partons all form separate subjets. So we have $O(e^Y)$ subjets each of a usable length in longitudinal rapidity that is $O(Y)$ units. Can we pick out a charge q that resides in one of these jets? Since each of these subjets is essentially one-dimensional we apply our charge measure to this collection of subjets, and find that the error on the measure is typically

$$\text{error} \sim \delta\left(e^Y/\sqrt{Y}\right) \xrightarrow[Y\to\infty]{} \infty \gg q \tag{44}$$

So we claim on the basis of these arguments (which could be strengthened by including the effects of $q\bar{q}$ production) that in a given QCD jet all charge information is lost as $Q^2 \to \infty$.

One should note that this statement only applies to a given jet. If for example we were to be provided with unlimited numbers of, say, u jets, then however, high the virtuality of the initial u quarks, we could always use enough jets for our average that the average net charge would give us the u quark charge (with the usual modifications of course) to arbitrarily good accuracy. It is amusing that the presence of the same perturbative showering makes it difficult to conceive of a source of quark jets, all of the same type, as $Q^2 \to \infty$.

5. Monte Carlo Studies

In this section we shall resort to a computer Monte Carlo simulation of QCD jets in order to study several questions which are too complicated to be addressed analytically.

The program we have used is that due to Fox and Wolfram (FW) [4]. This is based on the same perturbative branching view of jet development discussed in Sec. 3.

A highly virtual parton, initially off-shell by $Q^2 \lesssim O(S)$ initiates a branching process. As long as all the partons are off-shell by at least $Q_o^2 \sim 1\ \text{GeV}^2$, then $\alpha_s(Q^2) \lesssim 1$ and there is hope that a perturbative continuation of the branching makes sense. The branching is therefore allowed to continue until any given parton falls below Q_o^2 off-shell, at which point it decays no further.

In this way one arrives at a set of nearly on-shell partons whose subsequent

hadronization down to $Q^2 \sim \Lambda^2$, is controlled by the confinement mechanism.

The FW program in performing the branching actually samples kinematical regions outside the collinear or LLA approximation via the so-called Leading Pole Approximation [4] (LPA), which represents an improvement over use of collinear kinematics alone.

After branching the version of the program we have used splits final gluons into $q\bar{q}$ pairs, each quark is then connected by a string to its colour conjugate anti-quark to form colour-neutral pairs. The strings then decay to hadrons by a Feynman-Field cascade. (There exists a more refined version of the FW program where colour-singlet clusters are subsequently produced by combining nearest colour-neutral pairs, as necessary, and these then decay to hadrons.)

The hope is that in such a picture confinement is not a 'drastic' process. It involves quantum number redistribution only locally in phase space (cf assumption (ii) introduced in sec. 1 of SRCC). Hence hadronic multiplicity, and crucially for our purposes, charge structure, should be already largely determined at the colour-singlet 'pre-confinement' level. There are several a posteriori consistency checks which such a picture successfully satisfies [13].

Our main interest will lie in seeing how drastically perturbative jet evolution, which slows down the valence parton, degrades the accuracy of our optimal (for 'soft' jets) charge measure $Q_N(J)$. As we have seen in sec. 4 at truly asymptotic energies such an event-by-event measure fails altogether - but what about current PETRA energies, $\sqrt{S}$ = 30 GeV, where charge data is becoming available [12]?

We shall also be interested in whether current data should contain any particular charge structure signature of the posited underlying perturbative cascade mechanism. We shall argue that one such feature is the very strong expected correlation between jet multiplicity and leading charge structure. Other potentially clear-cut signatures such as sub-jet structure [3] should only become manifest around LEP energies.

To study these issues we have run the FW program with Q_o = 1 GeV and $\sqrt{S}$ = 30 GeV to produce two hundred single-jet events. The events are produced as $q\bar{q}$ 2-jet events with flavours u,d,s in the ratio of the squared electric charges. Events where the first gluon is hard and emitted at large angle, which are more naturally interpreted as 3-jet events, have been omitted by the imposition of a cut on initiating parton invariant mass; this is equivalent to a thrust cut on data. For our purposes, however, this cut will be largely irrelevant. We have also performed runs at some lower energies in order to study the variation of average charged hadron multiplicity. We have not included c,b flavours because of theoretical uncertainties concerning their decays. In general we would expect some degradation of all charge measures; in particular those involving only the fastest hadrons.

We start by discussing the general partonic structure of the FW jets.

General Partonic Structure of FW Quark Jets

The LLA prediction for the moments of the fractional energy of the valence quark after branching from Q^2 to Q_o^2 is, as we have seen in Sec. 3 [3] ,

$$\langle x_v^n \rangle = \exp\left(-A_n Y\right) \qquad (45)$$

In Fig. 5 we display the number density histogram, $\frac{dN}{dx_v}$, obtained from a sample of 200 events at $\sqrt{s}$ = 30 GeV, Q_o = 1 GeV. The distribution is strongly peaked towards $x_v = 1$ - about one quarter of the events lie in the fastest bin $.9 \leq x_v \leq 1$. If there were no perturbative branching we would have a $\delta(1 - x_v)$ spectrum prior to hadronisation.

The first few moments in x_v extracted from the FW data are: $\langle x_v \rangle = .67$, $\langle x_v^2 \rangle = .53(.53)$, $\langle x_v^3 \rangle = .45(.45)$. The bracketed figures represent the results obtained by fitting $\langle x_v \rangle$ from the LLA result (45) to obtain an effective value of Y (Y_{eff}). This value is then used to predict all the other moments. The agreement is clearly good. The effective value of Y is $Y_{eff} \simeq .23$, which at $\sqrt{s}$ = 30 GeV corresponds, in terms of LLA, to an effective cut-off Q_o = 1.7 GeV.

Thus the LPA gives less branching than the LLA. As we go to higher energies we expect collinear kinematics to become an increasingly good approximation. Thus the LLA and LPA results should become closer. To see this we have run the program at the LEP energy, $\sqrt{s}$ = 200 GeV, Q_o = 1 GeV. The $\frac{dN}{dx_v}$ histogram is given in Fig. 6.

Notice that the distribution has flattened out and become nearly uniform. We know that as $\sqrt{s} \to \infty$, $\frac{dN}{dx_v} \to \delta(x_v)$ and thus in evolving from the $\delta(1-x_v)$ form at low energy it must pass through such a flat stage before eventually becoming peaked at low x_v.

The FW results give $\langle x_v \rangle = .51$, $\langle x_v^2 \rangle = .34(.35)$. In this case we need $Y_{eff} = .375$, implying on effective cut-off Q_o = 1.3 GeV. Thus, as anticipated,

the effective cut-off is getting closer to the actual Q_o = 1 GeV as we increase the energy. The dashed curves in Figs. 5, 6 are numerical inversions of (52) at the values of Y_{eff} mentioned.

To give an intuitive feel for the partonic structure of the quark jet after branching at PETRA energy ($\sqrt{s}$ = 30 GeV) we shall give some further statistics extracted from FW results.

The average number of gluons at $Q_o^2 \lesssim 1$ GeV is ~ 2 per jet. On average the hardest secondary parton carries $x \sim .2$, and is (for events where branching has occurred) about 1 unit of rapidity below the valence parton.

Secondary $q\bar{q}$ pair production is negligible at PETRA energies - the average number of secondary quarks per jet is only about 0.1 and in only $\sim$ 15 % of cases where a $q\bar{q}$ pair occurs is either secondary quark the fastest parton in the jet. The rare $q\bar{q}$ pairs end up, on average, about 2 units of rapidity apart in longitudinal phase space. These results are in accord with our conclusion in Sec. 3 that the potentially disastrous consequences of $q\bar{q}$ pair production on our SRCC assumption (ii), are averted by the rarity of such production.

In Fig. 7 we plot the number density of secondary partons $\frac{dN}{dx}$. From the figure it can be seen that the density of secondary partons per unit rapidity is less than one, throughout the jet. Thus at PETRA energies our assumption (iii), that the density of hadrons per unit rapidity stays finite, should certainly be valid after hadronisation.

The parton structure of the jet should be directly mirrored in hadronic

features. Thus the increase in hadronic multiplicity with energy should be correlated with the increase in the amount of perturbative branching with energy and hence with the parton multiplicity at Q_o^2.

In Fig. 8 we display the average e^+e^- charged hadronic multiplicity, $\langle n_c \rangle$, versus $\sqrt{s}$ (logarithmic scale). The solid black points are experimental data points [14] and the open points and solid curve are the results of the FW Monte Carlo. The FW results are seen to be in good agreement with data except at the lowest energies, less than 5 GeV, where the near constancy of the multiplicity points to the importance of finite energy effects.

The line marked "$Q^2 = 0$" corresponds to the contribution to $\langle n_c \rangle$ of FW events where the initial q and $\bar{q}$ at the γ^* vertex are produced with $Q^2 < Q_o^2$ and hence no branching occurs. The fraction of such events tends to one as $\sqrt{s} \to 0$ and hence the "$Q^2 = 0$" line of logarithmic energy dependence characteristic of 'soft' jets, describes the low energy behaviour. As $\sqrt{s}$ increases the $\langle n_c \rangle$ curve increases faster than linear in ln$s$, the excess multiplicity being due to the increasing number of fragmenting partons at Q_o^2 produced through branching. At $\sqrt{s}$ = 30 GeV, for instance, we see from Fig. 8 that "$Q^2 = 0$" events contribute only half of the observed $\langle n_c \rangle$, thus perturbative branching serves to double the 'soft' jet expectation.

A Feynman-Field $q\bar{q}$ Monte Carlo model (dashed line in Fig. 8) can fit the higher energy data. This is purely fortuitous, however, since such a Monte Carlo takes no account of jet invariant mass and thus should have no contact with real data. It is also interesting to note that a $q\bar{q}g$ Monte Carlo taking account of large angle hard gluon bremsstrahlung via the $\gamma^* \to q\bar{q}g$ matrix element, gives the dashed-dotted line lying only marginally above

the FW (with its effective 2-jet cut) and Feynman-Field $q\bar{q}$ Monte Carlo predictions. Thus the increase in multiplicity is largely due to internal showering as opposed to large angle 3-jet production, as is often stated.

In the next section we shall turn to a discussion of how well our charge measures of (2) work for the FW results. We shall then dismantle these results to see in what way effects due to perturbative branching are present in the charge structure.

Charge Measures and the FW Results

We shall now consider how reliably the charge measure $Q_N(J)$ of (2) serves to distinguish a '+' QCD jet, i.e. $u,\bar{d},\bar{s}$ ... from a '−' QCD jet, $\bar{u},d,s$. As we discussed at length in (2) distinguishing between $u,\bar{d},\bar{s}$ is unlikely to be possible using only the charge measure, although some indirect means were proposed.

We shall examine the confidence level, $C(Q_N(J))$, with which the criterion $Q_N(J) \geqslant 0 \Rightarrow$ '+' jet, $Q_N(J) < 0 \Rightarrow$ '−' jet, allows one to identify $u,\bar{d},\bar{s}$ versus $\bar{u},d,s$ FW jets. We shall see later that such a confidence level, for a criterion which applies to all events, can be extracted from 2-jet e^+e^- data, where one has no prior knowledge of which jet is which.

We shall be concerned with $N = 1$ and $N = n_c$. The former measure is just equivalent to using the charge of the fastest charged hadron to identify the jet and has in its favour directness and lack of possible experimental ambiguity.

The FW results for our $\sqrt{s}$ = 30 GeV, Q_o = 1 GeV PETRA sample of 200 events are

$C(Q_1(J)) = .7 \pm .03$, $C(Q_{n_c}(J)) = .75 \pm .03$. From our naive model for 'soft' jets in (2) we would have estimated $C(Q_1(J)) = .67$, $C(Q_{n_c}(J)) = .8$ taking $n_c = \langle n_c \rangle = 6$. The agreement is reasonable. In both cases there is seen to be a significant improvement in confidence if one uses the full charged multiplicity of the jet as opposed to relying on the fastest charge alone.

Use of the combined 2-jet measure of (2): $\Delta Q(J_1,J_2) = \frac{1}{N}\left[N_1 Q_{N_1}(J_1) - N_2 Q_{N_2}(J_2)\right]$ with the criterion $J_1 = '+'$, $J_2 = '-'$ if $\Delta Q > 0$, or vice versa for $\Delta Q < 0$, gives $C(\Delta Q) = .8 \pm .04$ for FW jets. This is to be compared with a confidence of .7 if one identifies each jet of a 2-jet event using the fastest charge when these are opposite, and determines at random when the fastest charges are identical.

Having seen that our charge measure will correctly identify jets about 8 times out of 10 at upper PETRA energy we now turn to the signatures of perturbative branching contained in the charge structure.

6. Correlation Between Multiplicity and Charge Structure

The QCD perturbative branching responsible for the faster than logarithmic increase in $\langle n_c \rangle$ with energy, occurs only at the expense of slowing down the valence quark. Thus events with large n_c would be expected to have small x_v and vice versa.

To highlight the n_c/x_v correlation we plot in Fig. 9(a), (b) the fraction of FW events in each x_v bin which have below average (BA) and above average (AA) n_c. ($n_c < 6$ and $n_c \geq 6$ at $\sqrt{s} = 30$ GeV). As can be seen BA n_c is associated with large x_v, whilst AA n_c comes mostly from the central region in x_v where

there are more hard partons after branching, and tails-off slightly towards low x_v.

When the distributions of Fig. 9 are folded into the overall $\frac{dN}{dx_v}$ of Fig. 5, which is strongly peaked towards large x_v, we obtain the $\left(\frac{dN}{dx_v}\right)_{BA}$ and $\left(\frac{dN}{dx_v}\right)_{AA}$ distributions of Fig. 10(a), (b). $\left(\frac{dN}{dx_v}\right)_{BA}$ is a distribution more sharply peaked towards $x_v = 1$ than the overall spectrum, whilst $\left(\frac{dN}{dx_v}\right)_{AA}$ is a nearly flat distribution comparable to the overall spectrum at LEP energy of Fig. 6. Thus even at PETRA energies above and below average multiplicities correspond to drastically different underlying x_v spectra.

The slowing down of the valence quark by perturbative branching will in principle reduce the effectiveness of an event-by-event charge measure such as our $Q_N(J)$, because it will dilute our assumption (i) of Sec. 1, that the valence parton ends up in a fast hadron after the ensuing hadronisation. To study this effect we plot in Fig. 11 the confidence level $C(Q_N(J))$ for each x_v bin, versus x_v. The solid histogram represents $N = n_c$ where we use the full charged multiplicity of the jet, and the dashed one $N = 1$ where we use the fastest charge. In both cases the confidence tails off to .5, i.e. random, as $x_v \to 0$ as we should expect, and increases to .9, .8 for the fastest x_v bin where there is little branching. Notice that use of the full hadronic multiplicity results in much higher confidence, at large x_v, than use of the fastest charge alone.

If we fold this distribution into the sharply peaked $\left(\frac{dN}{dx_v}\right)_{BA}$ distribution of Fig. 10(a) we weight up the confidences at large x_v and obtain $C(Q_1(J))_{n_c<6} = .76 \pm .04$ (cf. .7 $\forall$ events) and $C(Q_{n_c}(J))_{n_c<6} = .79 \pm .04$

(cf. .75 ∀ events) which are very much higher confidence values than we obtain for below average multiplicity by folding in the flat $\left(\frac{dN}{dx_v}\right)_{AA}$ distribution of Fig. 10(b) which will average over confidences at all x_v values - $C(Q_1(J))_{n_c \geq 6} = .64 \pm .04$ and $C(Q_{n_c}(J))_{n_c \geq 6} = .69 \pm .04$.

Thus the fact that x_v is strongly correlated both with n_c and C(Q) means that there is a large difference between the confidence level at which the charge measure operates for above average and below average charge multiplicities. In a 'soft' picture of hadronisation, without QCD branching, there will only be a very weak effect of this kind due to the larger rapidity density for above average multiplicity events. Thus the observation of this strong charge structure-multiplicity correlation in present PETRA data would be indicative of underlying perturbative branching.

In the next section we shall indicate how the single-jet confidence levels $C(Q_N(J))$ can indeed be extracted from 2-jet e^+e^- data and we shall also mention that use of the actual charge permutation of the jet particles, supplemented with Monte Carlo studies, should provide a truly optimum charge measure.

7. Extraction of $C(Q_N(J))$ and the optimum Measure

$C(Q_N(J))$ is easily extracted from a sample of 2-jet events by measuring the average

$$P(Q_N(J)) = -\left\langle \bar{Q}_{N_1}(J_1)\bar{Q}_{N_2}(J_2)\right\rangle$$

where the product is taken for each two-jet event and

$$\bar{Q}_N(J) = \begin{cases} 1 & Q_N(J) \geq 0. \\ -1 & Q_N(J) < 0. \end{cases}$$

It is then trivial to show that

$$C(Q_N(J)) = \frac{1}{2} + \frac{\sqrt{P(Q_N(J))}}{2}$$

By measuring the analogue of P for different charge measures, for example the Feynman-Field Z-weighted charge sum [6], and our own $Q_N(J)$, one can then obtain from 2-jet e^+e^- data an objective assessment of how well these event-by-event measures work relative to each other. This is preferable to measuring $-\left\langle Q(J_1)Q(J_2)\right\rangle$ for the measure itself, which has already been done in [12] for the Feynman-Field measure, because this average depends on the shape of the distribution in the charge measure, as opposed to how well it differentiates between jets of different underlying charge, which is what we are interested in.

Using $P(Q_N(J))$ on $\sqrt{S}$ = 30 GeV PETRA data the FW results would predict:

$$P(Q_1(J)) = .16 \pm .05$$
$$P(Q_{n_c}(J)) = .25 \pm .06$$
$$P(Q_1(J))_{AA} = .08 \pm .05$$
$$P(Q_1(J))_{BA} = .27 \pm .09$$
$$P(Q_{n_c}(J))_{AA} = .14 \pm .07$$
$$P(Q_{n_c}(J))_{BA} = .34 \pm .09$$

Here P_{BA}, P_{AA} denote the average over two-jet events where both jets have respectively below average or above average charged multiplicity. The experimental observation of the predicted big difference between P_{AA} and P_{BA} would, as explained earlier, be a strong indication of the presence of perturbative branching in the PETRA jets.

Of course, for neutrino or antineutrino production, where the flavour of the final current quark is fixed one can measure the confidence levels directly.

We finally make some remarks concerning the optimum charge measure. It is clear that we can do rather better than using $Q_N(J)$ to decide the underlying charge. $Q_N(J)$ only depends on the sequence of charges ordered in rapidity. For N charged particles there are 2^N such permutations. For instance N = 2 has ++ , -- , +- , -+ as the 4 permutations. By studying a large sample of Monte Carlo events one could, in principle, determine the probability p(P) that the permutation P results from a '+' QCD jet, 1-p(P) that it results from a '-' QCD jet. If $p(P) > \frac{1}{2}$ then any jet having charge permutation P should be identified as '+' or vice-versa for $p(P) < \frac{1}{2}$.

Such a procedure is guaranteed, since it utilizes all available information, to work with a better confidence level than $Q_N(J)$ which can assign the same value of measure to two different permutations.

8. Conclusions

In this paper we have conducted a detailed investigation of the effects of perturbative branching upon our ability to decide from the charge structure of the hadrons in a given QCD jet the charge of the initial QCD quantum:

in particular within the context of a charge measure which we had shown earlier [2] to be insensitive to the charge fluctuations incurred during the final soft hadronisation.

Our numerical calculations at the highest currently available energies of about 30 GeV were perforemed using the Monte Carlo program of Fox and Wolfram. We found that in a typical 2 jet event at such an energy our charge measure would correctly identify the $u\bar{u}$ (for example) orientation some 80 % of the time. This is close to our previous, naive estimates in ref. (2) and is a significant improvement on the 70 % obtained by using only the leading charges in each jet.

We made some asymptotic analytic estimates. In particular we explicitly evaluated our charge measure for a jet of virtuality $\sim 10^{15}$ GeV, and the charge identification was found to have become poor by this energy (which is the highest of any possible physical interest in pure QCD).

We showed that as $Q^2 \to \infty$ all charge information is lost on an event by event basis; not just with our charge measure, but with any charge measure.

Finally we pointed out that the variation of the multiplicity at a given energy is strongly correlated to the amount of the perturbative showering in a given jet, and that this is sensitively reflected in the charge structure of the jets.

Acknowledgements

We gratefully acknowledge John Babcock's extensive work on the Monte Carlo program we have employed, without which it could not have been used by us. We thank Ken Konishi and Stephen Wolfram for discussions and Professor Joos for reading the manuscript. One of us (M.T.) would like to thank the Theory Group at the Rutherford Laboratory for its hospitality and financial support at various times during the course of this work.

References

1) M.J. Teper, Phys. Lett. 90B (1980) 443.

2) C.J. Maxwell, M.J. Teper, Zeitschrift für Physik C (1981)

3) K. Konishi, A. Ukawa, G. Veneziano, Nuclear Physics B157 (1979) 45.
K. Konishi, CERN preprint TH 2853, April 1980 (and references therein).

4) The Monte Carlo is described in
G.C. Fox and S. Wolfram, Caltech Preprint CALT-68-755 (1979).

5) S. Wolfram, Rencontre de Moriond, (1980).
R.D. Field and S. Wolfram, "QCD Models for hadron production in e^+e^- annihilation", CALT- preprint (1980)

6) For some alternative measures see:
R.D. Field and R.P. Feynman, Nucl. Phys. B136 (1978) 1.

7) M.J. Teper, preprint DESY 81-007.

8) J.P. Berge et al., Phys. Lett. 91B (1980), 311.
N. Schmitz, Lectures at the XX Krakow School, Zakopane, June 1980, MPI-PAE/Exp. E1.88.

9) A. Bassetto, M. Ciafaloni, G. Marchesini, Nucl. Phys. B163, 477 (1980).

10) K. Konishi, private communication.

11) For example:
Le Bellac, CERN yellow report: 76-14, Aug. 76 and references therein.

12) TASSO collaboration: DESY preprint 81-005
W. Koch, seminar at DESY, December 1980

13) G. Marchesini, L. Trentadue, G. Veneziano, CERN preprint TH 2924 (1980)

14) 'Jets in e^+e^- Annihilation', G. Wolf, DESY preprint 80-85 (1980)

Figure Captions

Fig. 1 The jet of hadrons, plotted against rapidity and transverse momentum, is partitioned into boxes whose linear dimension is the charge correlation length l_c. The jet is effectively one-dimensional so that its transverse dimension is less than l_c. The initial quark typically will be in the first box, and the charge flowing across the i'th face will be some antiquark charge plus some random charge fluctuation σ (i) as shown.

Fig. 2 The number of secondary partons with virtuality $Q_o^2 \sim 1$ GeV^2, and with momentum greater than the average final momentum of the initial quark, is plotted versus the variable Y (see text). Energies corresponding to PETRA, LEP and GUTS are indicated.

Fig. 3 The square root of the number of partons with virtuality $Q_o^2 \sim 1$ GeV^2 per unit rapidity interval is plotted versus the rapidity (y = 0 corresponds to the rapidity of the incident quark) for a quark jet where the incident quark has a virtuality $\sim 10^{15}$ GeV. This also equals the quantity $\beta\sigma$ - see text.

Fig. 4 A jet of hadrons at large Q^2 where transverse momenta have become large, although still small compared to the longitudinal momenta. The jet is plotted against longitudinal rapidity y, and transverse rapidity, $y_\perp \sim \frac{1}{2} \ln (m^2 + p_\perp^2)$, and is partitioned into boxes of dimension l_c. In contrast to the soft jet in Fig. 1, the jet now possesses non-trivial transverse structure.

Fig. 5 Valence quark distribution after branching down to $Q_o^2 = 1$ GeV at $\sqrt{s} = 30$ GeV, extracted from 200 events of FW Monte Carlo. The dashed curve shows the LLA expectation at the Y value which fits the $\langle x_v \rangle$ of the distribution.

Fig. 6 As Fig. 5 but $\sqrt{s} = 200$ GeV.

Fig. 7 Number density of secondary partons at $\sqrt{s} = 30$ GeV, $Q_o^2 = 1$ GeV^2. Extracted from FW results.

Fig. 8 Average hadronic charged multiplicity vs $\sqrt{s}$. The black points are selected e^+e^- data (see ref. 14). The open points and solid curve are FW results. The "$Q^2 = 0$" line is the FW expectation with no branching. The dashed line is a Feynman-Field $q\bar{q}$ Monte Carlo expectation, and the dashed-dotted is the $q\bar{q}g$ expectation.

Fig. 9 (a), (b). Fraction of $\sqrt{s} = 30$ GeV FW events in each x_v bin having, respectively, $n_c < 6$ and $n_c \geq 6$.

Fig. 10 (a), (b) x_v distribution corresponding to $n_c < 6$ and $n_c \geq 6$ respectively.

Fig. 11 Confidence level $C(Q_N(J))$ for each x_v bin. N = n_c (solid line), N = 1 (dashed line).

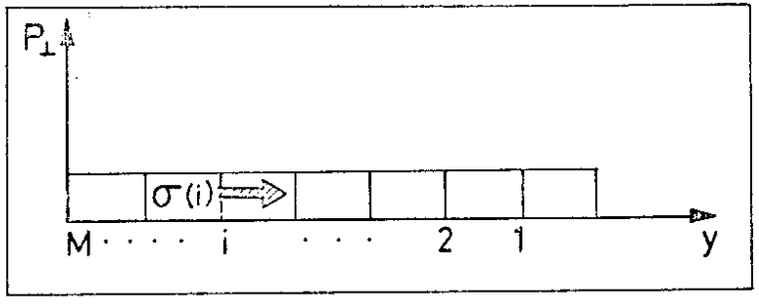
$P_\perp$
$\sigma(i)$
M · · · · i · · · 2 1 y

Fig.1

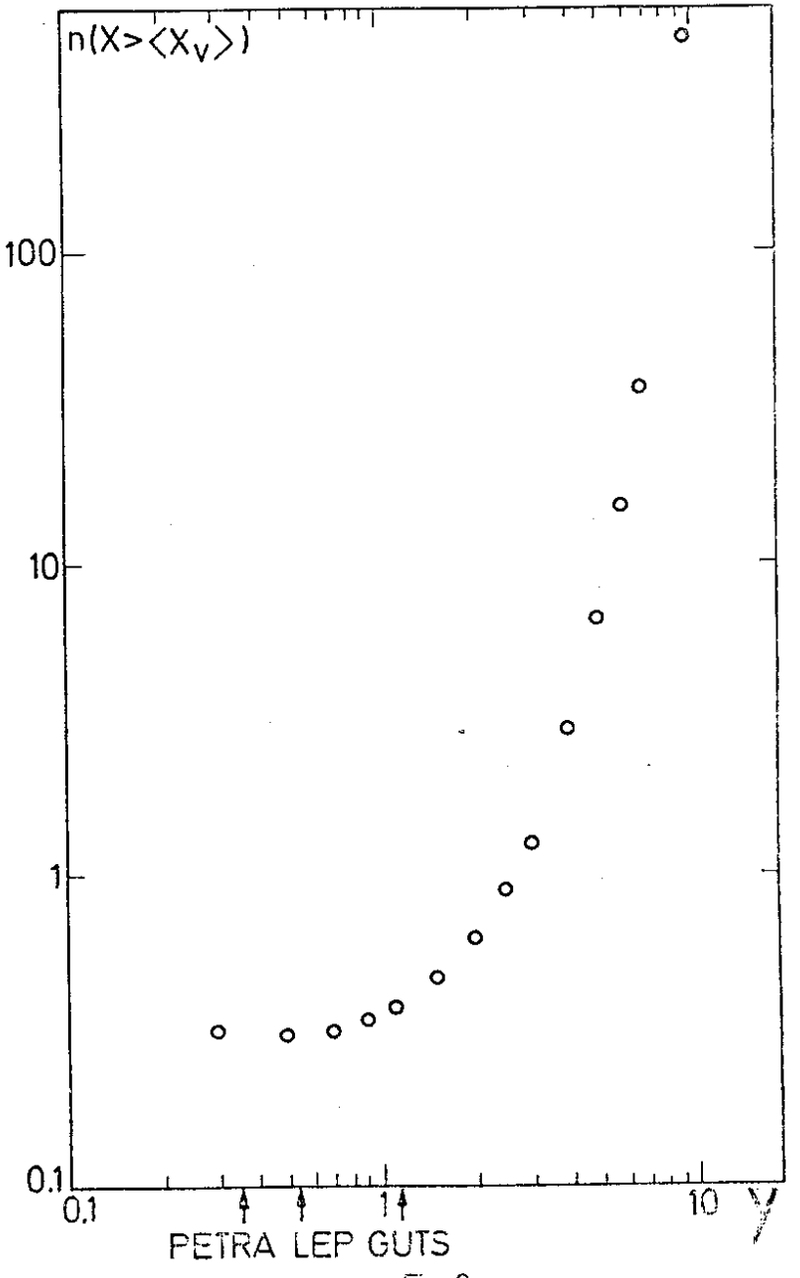
$n(X>\langle X_v\rangle)$
100
10
1
0.1
0.1
1
10
y
PETRA LEP GUTS

Fig.2

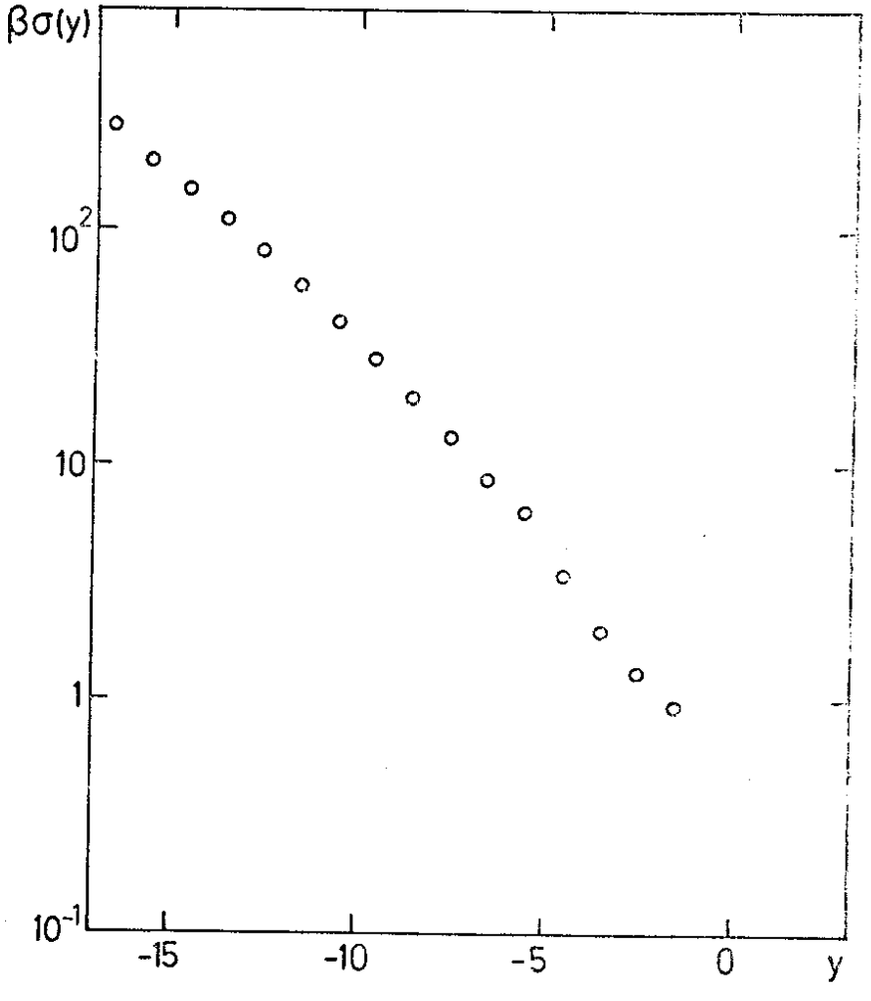

Fig.3

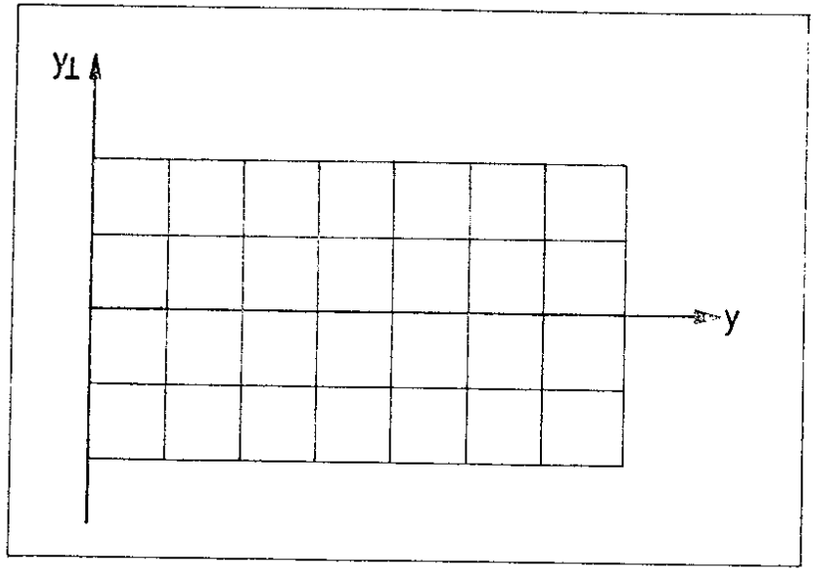

Fig.4

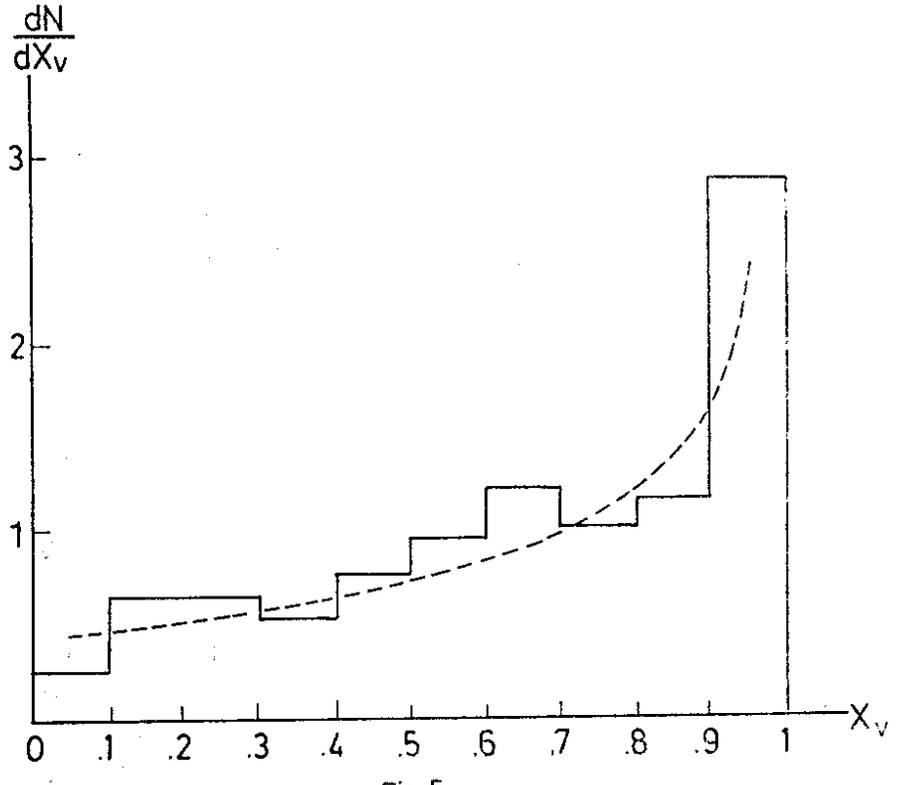

Fig.5

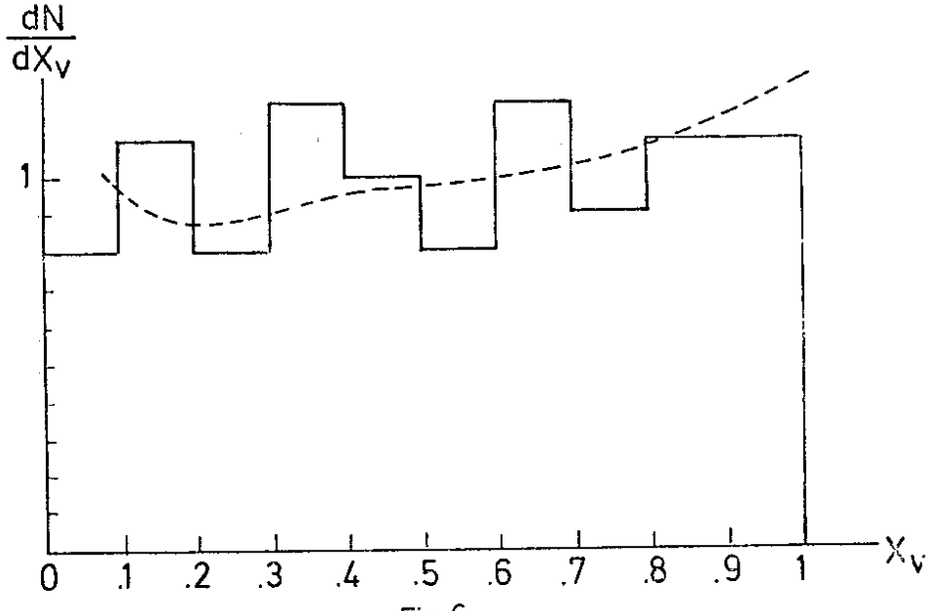

Fig.6

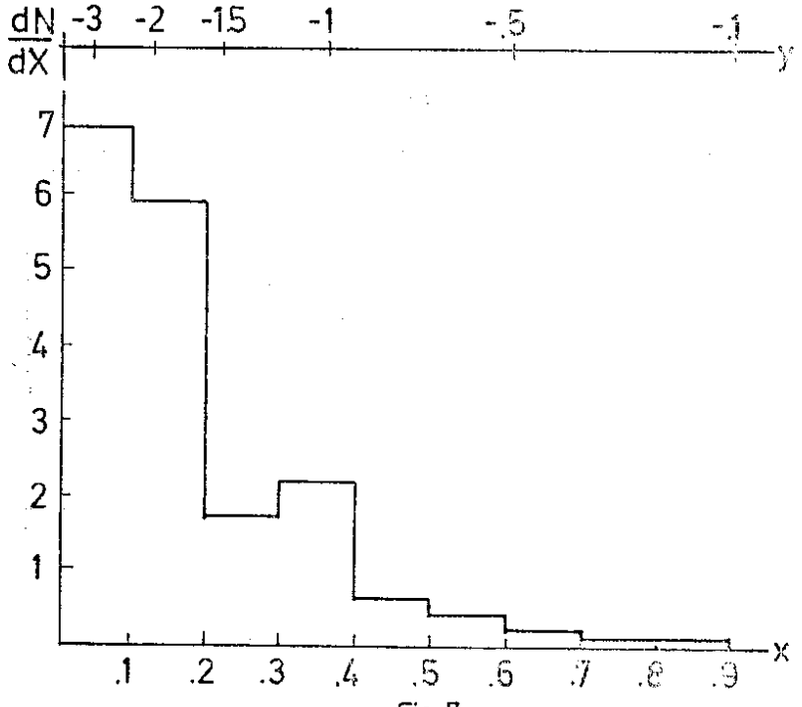
dN/dX
-3
-2
-15
-1
-.5
-.1
y
7
6
5
4
3
2
1
.1
.2
.3
.4
.5
.6
.7
.8
.9
x

Fig.7

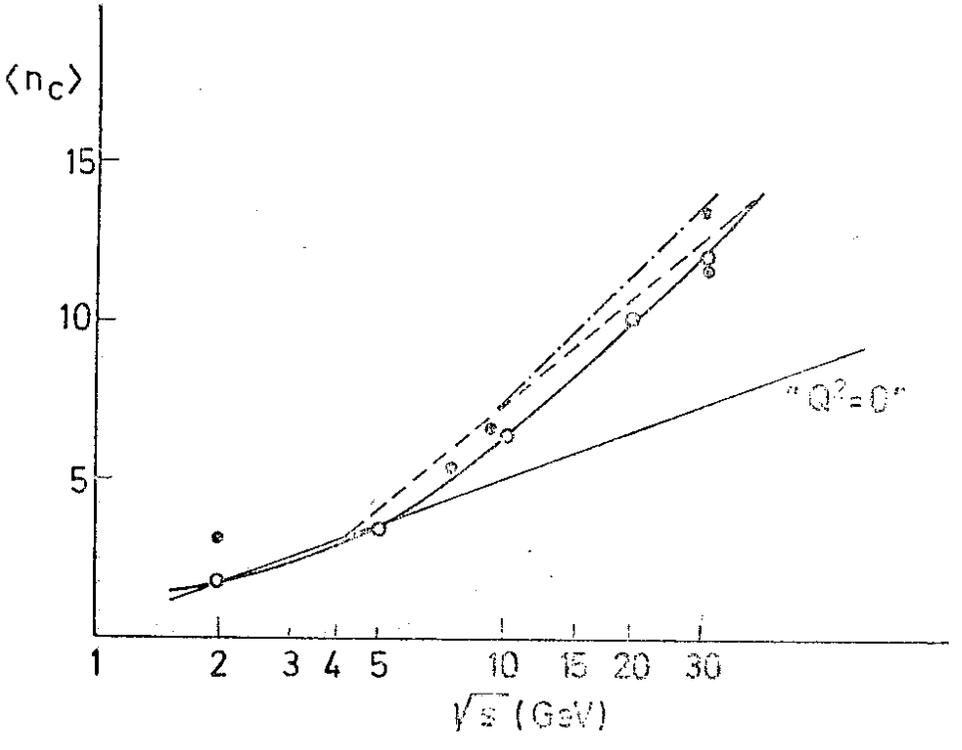
⟨nc⟩
15
10
5
1
2
3
4
5
10
15
20
30
√s (GeV)
"Q²=0"

Fig.8

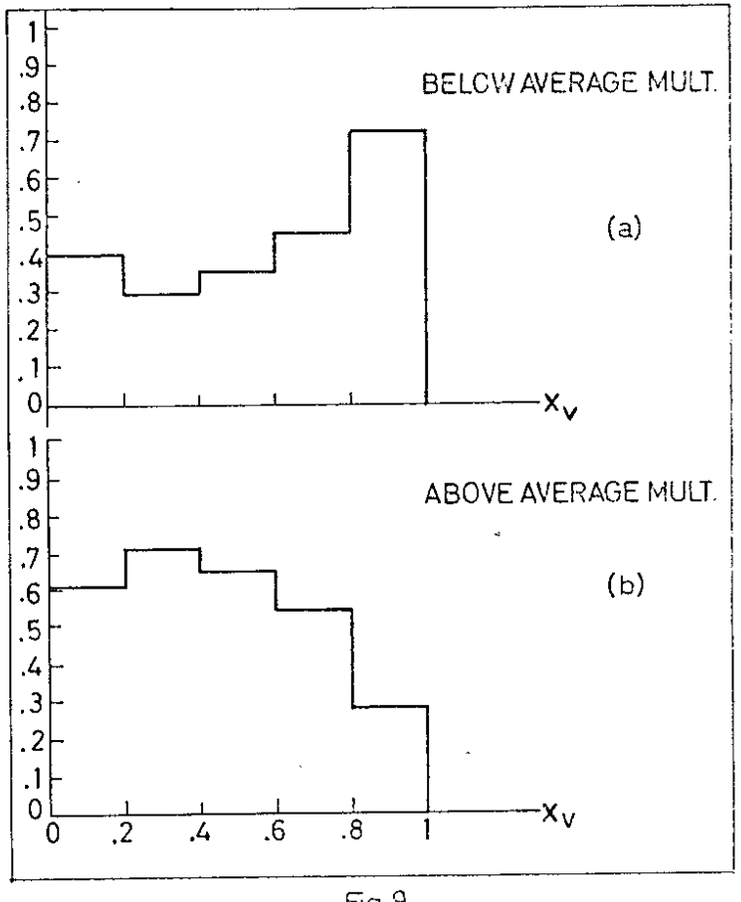

Fig.9

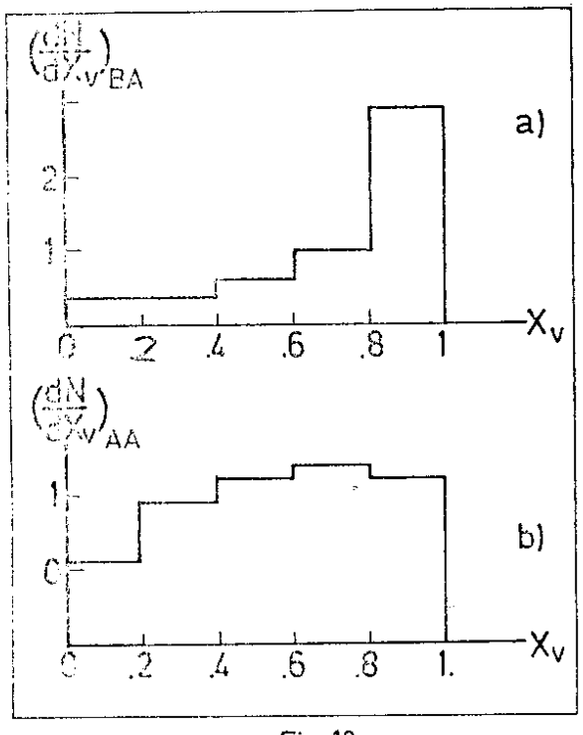

Fig.10

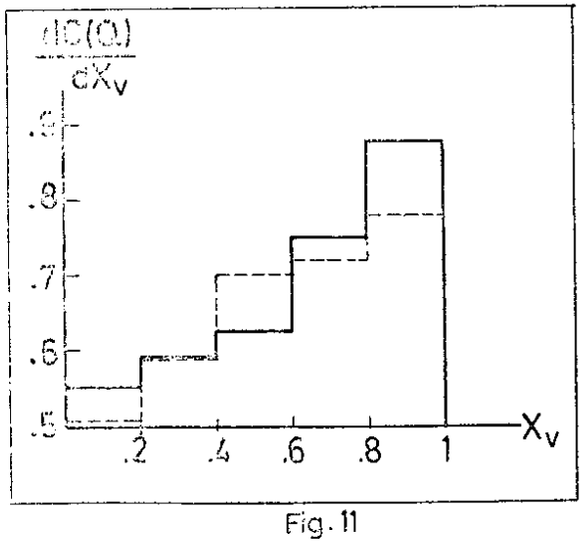

Fig. 11